Supplementary Material for

The unexpectedly short Holocene Humid Period in Northern Arabia

Ina Neugebauer[1,2], Michèle Dinies[3,4], Birgit Plessen[1], Nadine Dräger[1], Achim Brauer[1], Helmut Brückner[5], Peter Frenzel[6], Gerd Gleixner[7], Philipp Hoelzmann[4], Kim Krahn[8], Anna Pint[6], Valérie F. Schwab[7], Anja Schwarz[8], Rik Tjallingii[1] and Max Engel[9,10,*]

1 GFZ German Research Centre for Geosciences, Section Climate Dynamics and Landscape Evolution, Telegrafenberg, 14473 Potsdam, Germany

2 University of Geneva, Department of Earth Sciences, Rue des Maraichers 13, 1205 Genève, Switzerland

3 German Archaeological Institute (DAI), Scientific Department of the Head Office, Im Dol 2-6, 14195 Berlin, Germany

4 Freie Universität Berlin, Institute of Geographical Sciences, Malteser Str. 74-100, 12249 Berlin, Germany

5 University of Cologne, Institute of Geography, Zülpicher Str. 45, 50674 Köln, Germany

6 Friedrich Schiller University Jena, Institute of Earth Sciences, Burgweg 11, 07749 Jena, Germany

7 Max Planck Institute for Biogeochemistry, Research Group Molecular Biogeochemistry, Hans-Knöll-Str. 10, 07745 Jena, Germany

8 Technische Universität Braunschweig, Institute of Geosystems and Bioindication, Langer Kamp 19c, 38106 Braunschweig, Germany

9 Heidelberg University, Institute of Geography, Im Neuenheimer Feld 348, 69120 Heidelberg, Germany

10 Royal Belgian Institute of Natural Sciences, Geological Survey of Belgium, Jennerstraat 13, 1000 Brussels, Belgium

* Corresponding author: Max Engel, max.engel@uni-heidelberg.de

Supplementary Note 1: Regional setting of Tayma and its sabkha

The sabkha north of the town of Tayma fills a closed basin overlying Lower Ordovician micaceous siltstones (Qasim Formation), with an extension of approximately 20 km^2 and a hydrological catchment 660 km^2[1,2] (Supplementary Fig. 1). Today, the deepest point of the sabkha is at about 800 m a.s.l. (above sea level). Here, at the bottom of the sabkha, the groundwater table is only 0.5 to 1.5 m b.s. (below surface) based on measurements from numerous boreholes (Supplementary Fig. 1a). The relatively small catchment leads to shallow flooding of the sabkha for days to several weeks after rare, episodic rainfall events[3], when surface discharge provides clastic sediment input. In case of a high groundwater table, that is controlled by recharge of the Saq aquifer (Fig. 1b), aeolian sediments may be trapped at the surface and incorporated into the halite and gypsum buckled crust. Drying of the surface after a fall of groundwater level leads to predominant deflation. The capillary fringe above the phreatic zone is dominated by evaporites precipitated from ascending groundwater, mostly gypsum, plugging the pore space[4]. With the shallow groundwater table very close to the surface, an increase in annual precipitation such as during the Holocene Humid Period (HHP) will inevitably have led to infill of the basin and permanent lacustrine conditions. In these conditions, sedimentation is dominated by authigenic deposition of evaporites, organic matter, diatoms, minor amounts of clastic sands to clays periodically introduced by debouching wadis (Supplementary Fig. 1a,b, 3a), as well as minor input of aeolian sand, as described in detail in refs[1,4,5].

The depression developed in a Northwest-Southeast-trending graben structure above the Ordovician Qasim Formation (Supplementary Fig. 1c). The Northern rim consists of an escarpment of steep, slightly Northwards dipping sandstones and micaceous siltstones of this formation. They have a maximum height at about 860 m a.s.l. (Supplementary Fig. 1a) and form part of an escarpment system covering large parts of the central Arabian Peninsula[6]. To the South, the surface gradually rises towards the town situated above the basin at about 830 m a.s.l., from where the underlying Ordovician Saq sandstone continuously rises up to 1000 m a.s.l. These about 600 m-thick medium to coarse-grained sandstones form the main groundwater-bearing layer of the Western Peninsula, the Saq aquifer[7] (Supplementary Fig. 1c). The groundwater flow coming from the Southeast[8] is under artesian pressure due to the graben structure of the Tayma basin. Potential surface waters drain by several small inflows and wadis into the endorheic basin (Supplementary Fig. 1b), some of which are mentioned in the works of historical Arabic geographers. Al-Bakri, reporting from the 11th century AD, mentions the wadi “Fayha River” reaching the oasis and entering the sabkha – referred to as a “lake” (*al-Aqirah*) – from the South, “which carried rain-water to Tayma” and “might have been added by water from a spring or another resource outside Tayma”[9].

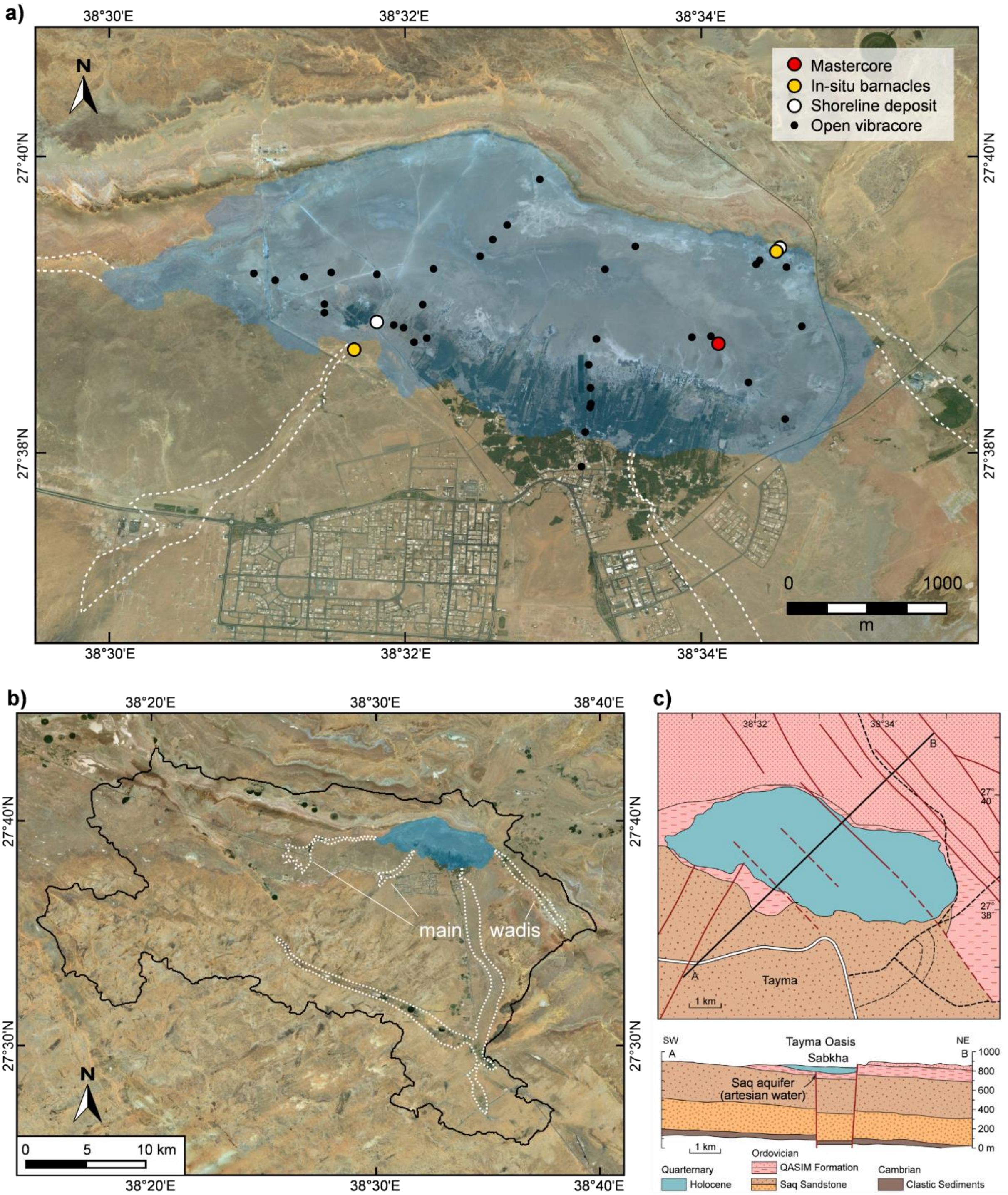

Supplementary Fig. 1: Local setting of the Tayma palaeolake. (a) Tayma palaeolake as reconstructed from highest shoreline deposits[1], a digital elevation model based on local DGNSS and global SRTM data[2] and a large dataset of vibracores (basemap: Landsat/Copernicus, accessed through Google Earth Pro). The main wadis entering the endorheic basin are marked by white dashed lines. (b) Surface catchment of the Tayma palaeolake[10] showing the spatial extent of the main wadis (basemap: Landsat/Copernicus, accessed through Google Earth Pro). (c) Simplified geology and tectonic features of the oasis of Tayma creating the artesian groundwater source, shown as top view and stratigraphic profile based on ref.[11].

Supplementary Fig. 2: Views of the sabkha of Tayma. (a) Panoramic view from the Northwestern margin on top of the lowermost escarpment towards Southeast, overlooking the sabkha. Zeugenbergs in the upper left represent remnants of higher escarpment levels. The upper right shows the palm gardens bordering the sabkha in the South as well as some buildings of the Easternmost part of the oasis of Tayma. (b) Typical gypsum buckled-crust surface of the central part of the sabkha, thinly covered by Na^+ salts. (c) In some more central parts, the buckled crust gives way to massive salt polygons.

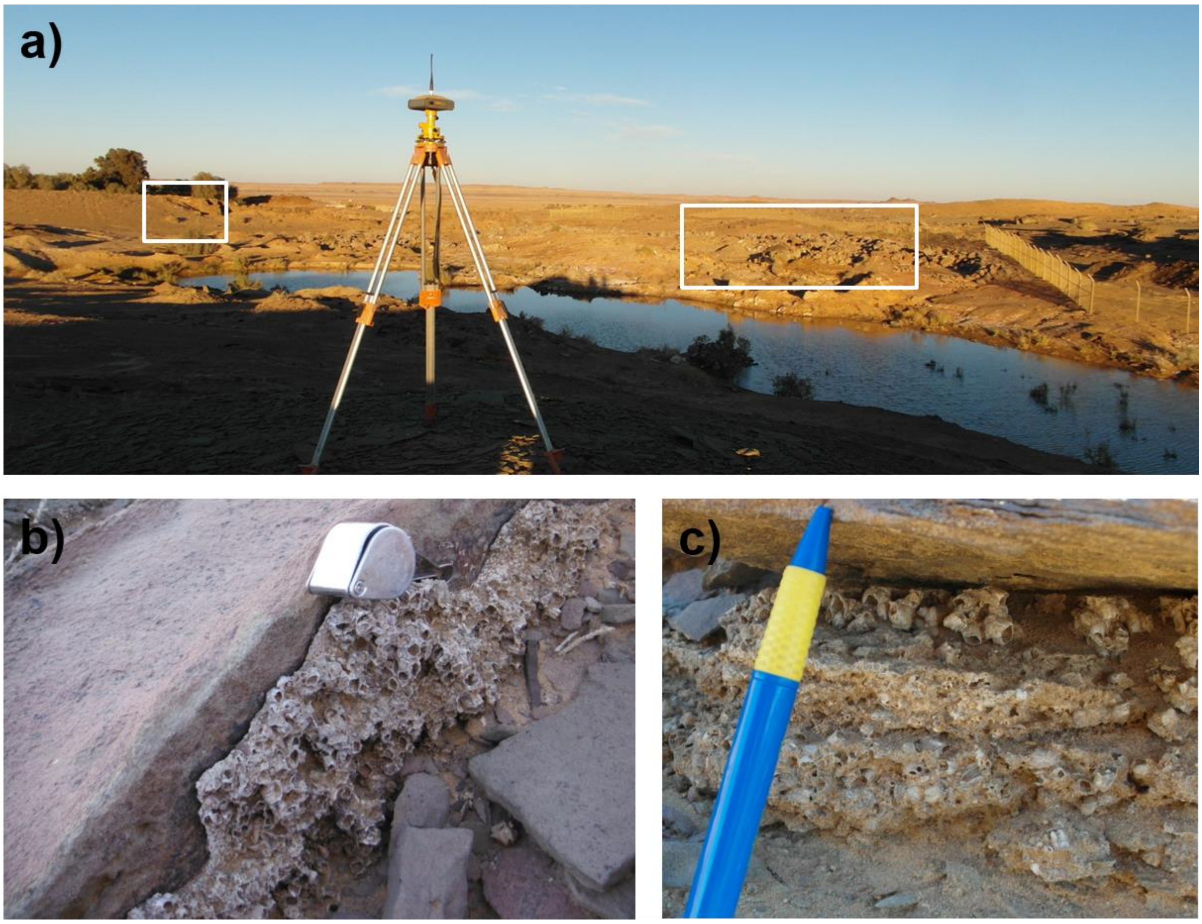

Supplementary Fig. 3: Southwestern barnacle colonies. (a) Overview of the Southwestern major wadi entering the sabkha basin (Supplementary Fig. 1a). (b), (c) Along both wadi margins, *in-situ* Holocene barnacle colonies are preserved at elevations of ca. 12 m above the present sabkha floor, representing palaeo-shoreline indicators of the peak phase of the early to mid-Holocene lake (Southwestern yellow dot in Supplementary Fig. 1a).

Supplementary Fig. 4: Southwestern bioclastic deposit. (a) Stratified lake-shoreline deposit almost entirely consisting of barnacles, gastropod, ostracod and foraminifer shells and tests, as well as quartz sand (thickness ca. 2.3 m; Southwestern white dot in Supplementary Fig. 1a). Shells were dated to the early Holocene (profile TAY 180 in refs.[1,5]). (b) *In-situ* barnacles attached to local Ordovician siltstone clasts floating in the bioclastic matrix. (c) Close-up of the texture in (a).

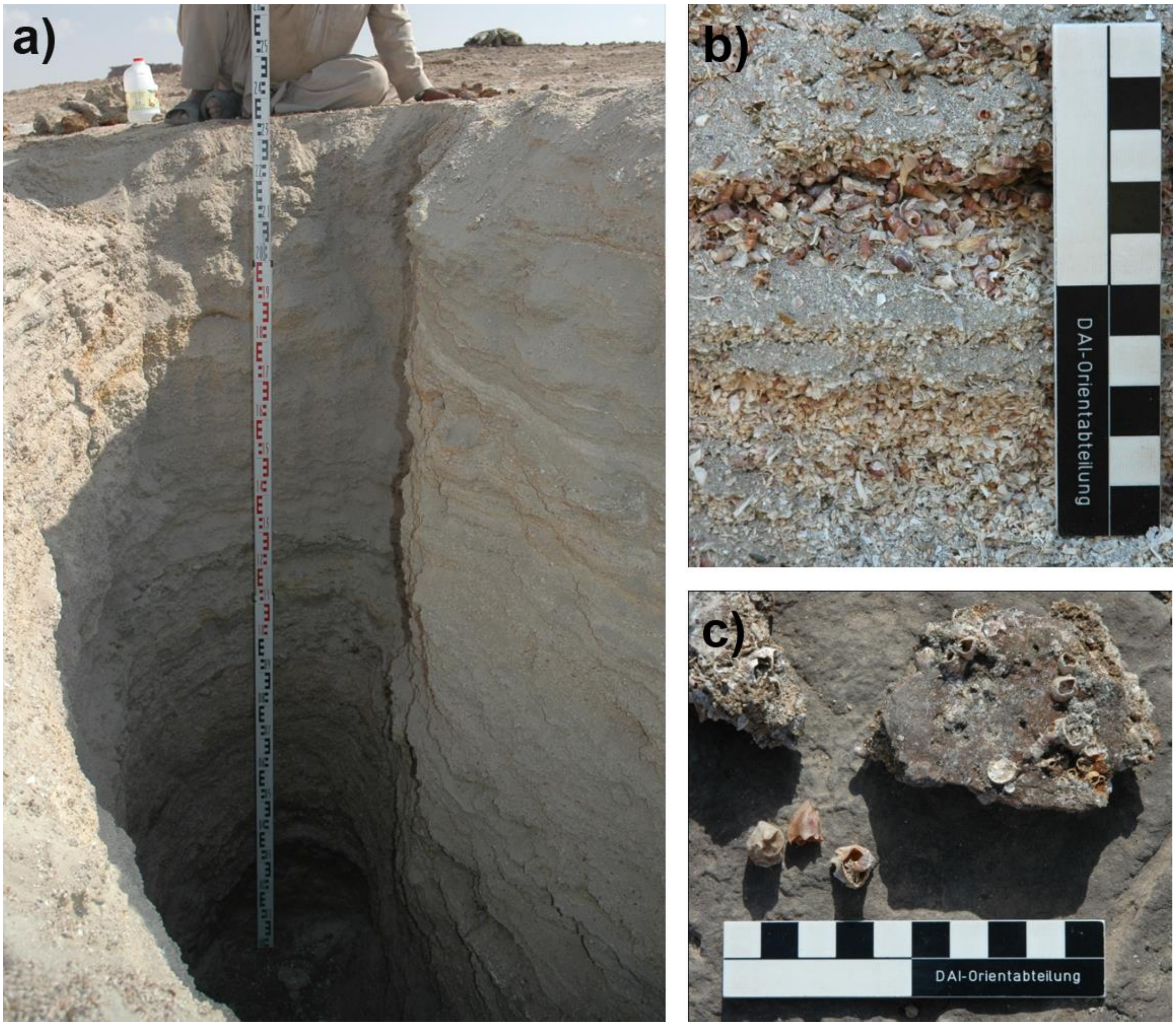

Supplementary Fig. 5: Northeastern bioclastic deposit. (a) Stratified lake-shoreline deposit almost entirely consisting of barnacles, gastropod, ostracod and foraminifer shells and tests, as well as quartz sand (Northeastern yellow and white dots in Supplementary Fig. 1a). Shells were dated to the early Holocene (profile TAY 177 in ref.[1]). (b) Close-up of the texture in (a). (c) *In-situ* Holocene barnacles attached to local Ordovician siltstone at the base of the profile.

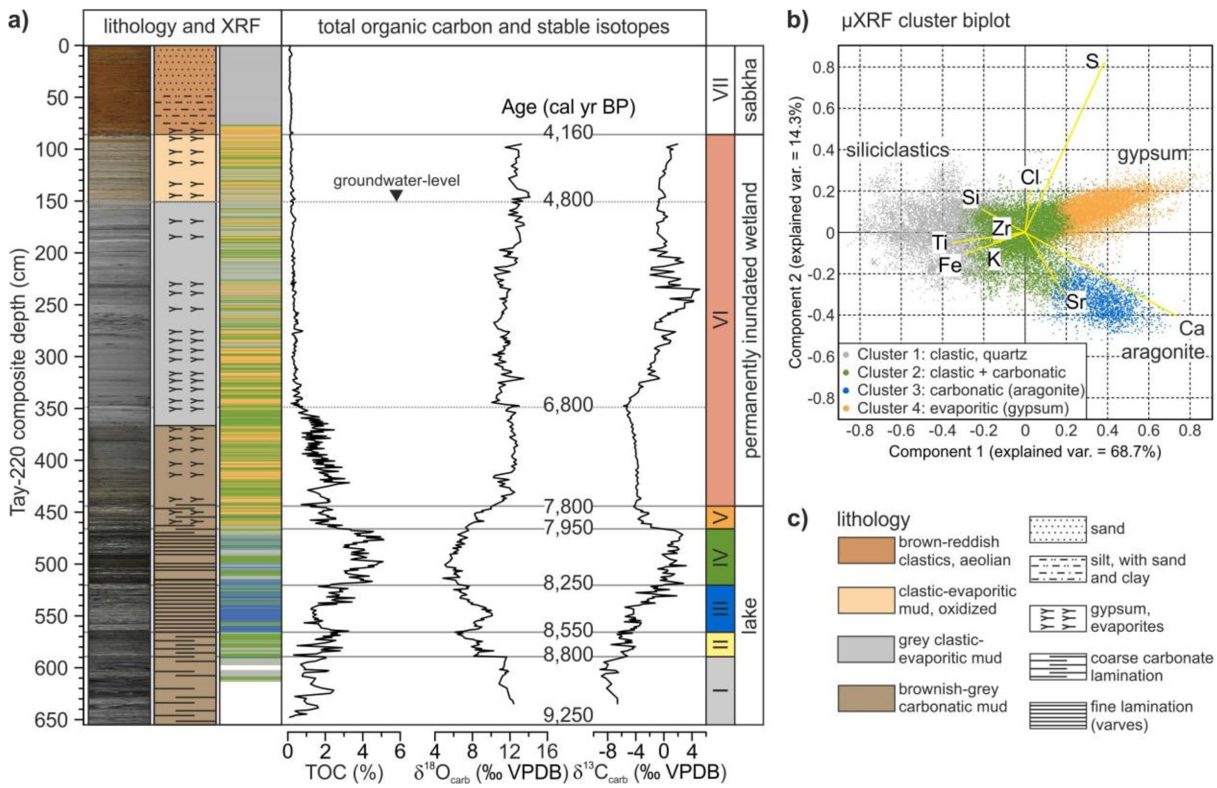

Supplementary Fig. 6: Lithology and sediment geochemistry of the Tayma composite profile. (a) Core scans, lithological description, down-core clustering results from XRF elemental scanning data (see (b) for legend), total organic carbon content (TOC)[12], $\delta^{18}O_{carb}$ and $\delta^{13}C_{carb}$ stable isotopes data, and discrimination of lake phases; the recent (in 2015) groundwater level at 1.5 m depth is marked with black triangles. (b) Principal-component biplot of XRF core-scanning results showing the statistical clusters; principal components 1+2 explain 83% of the variance. (c) Legend for the lithological description.

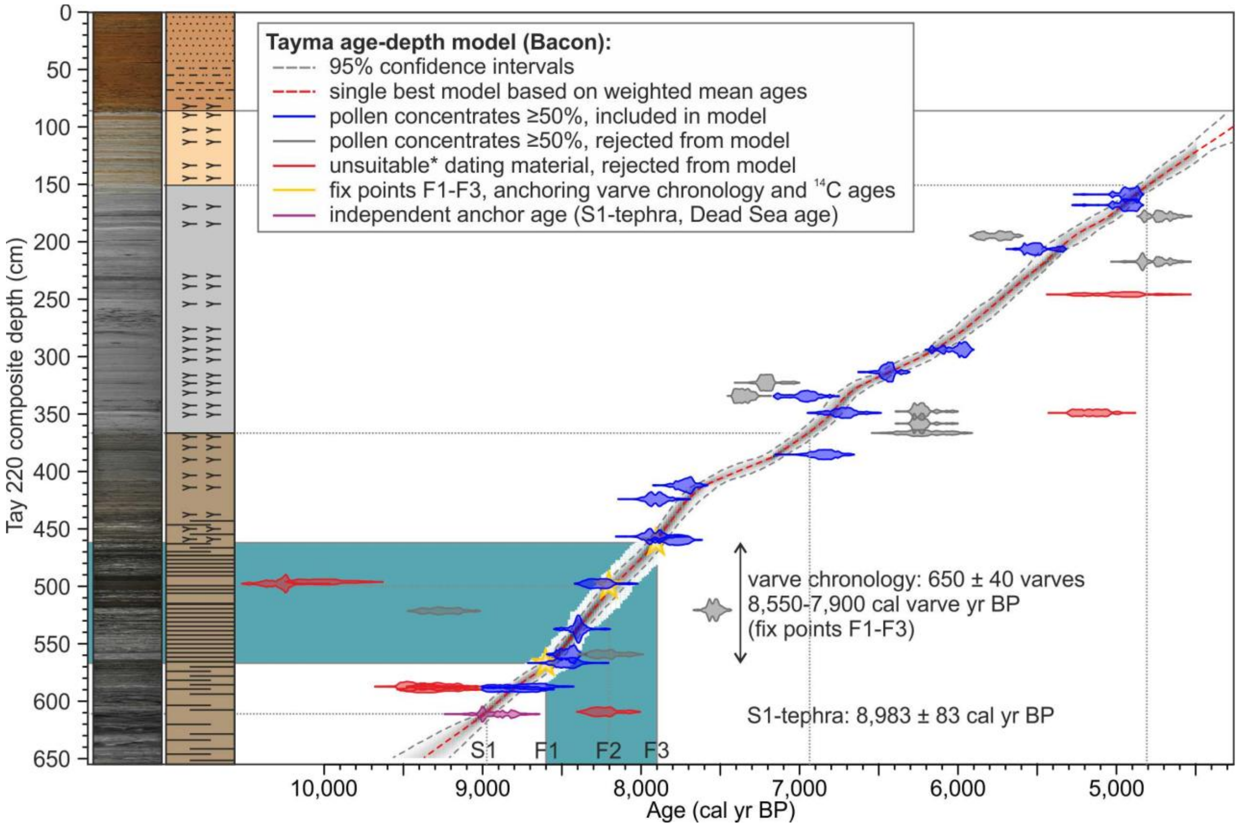

Supplementary Fig. 7: Age-depth model of the Tayma sediment composite profile. The age-depth model was constructed with Bacon v2.2 using flexible Bayesian modelling[13] including implemented outlier analysis and the IntCal13 atmospheric calibration curve[14] (see Methods). The model is based on radiocarbon ages of pollen concentrates (Supplementary Data 1), an independent anchor age of the S1 tephra[15] and a varve chronology between 8,550 and 7,900 cal varve yr BP (Tayma deep-lake phases III and IV; marked with a blue rectangle).

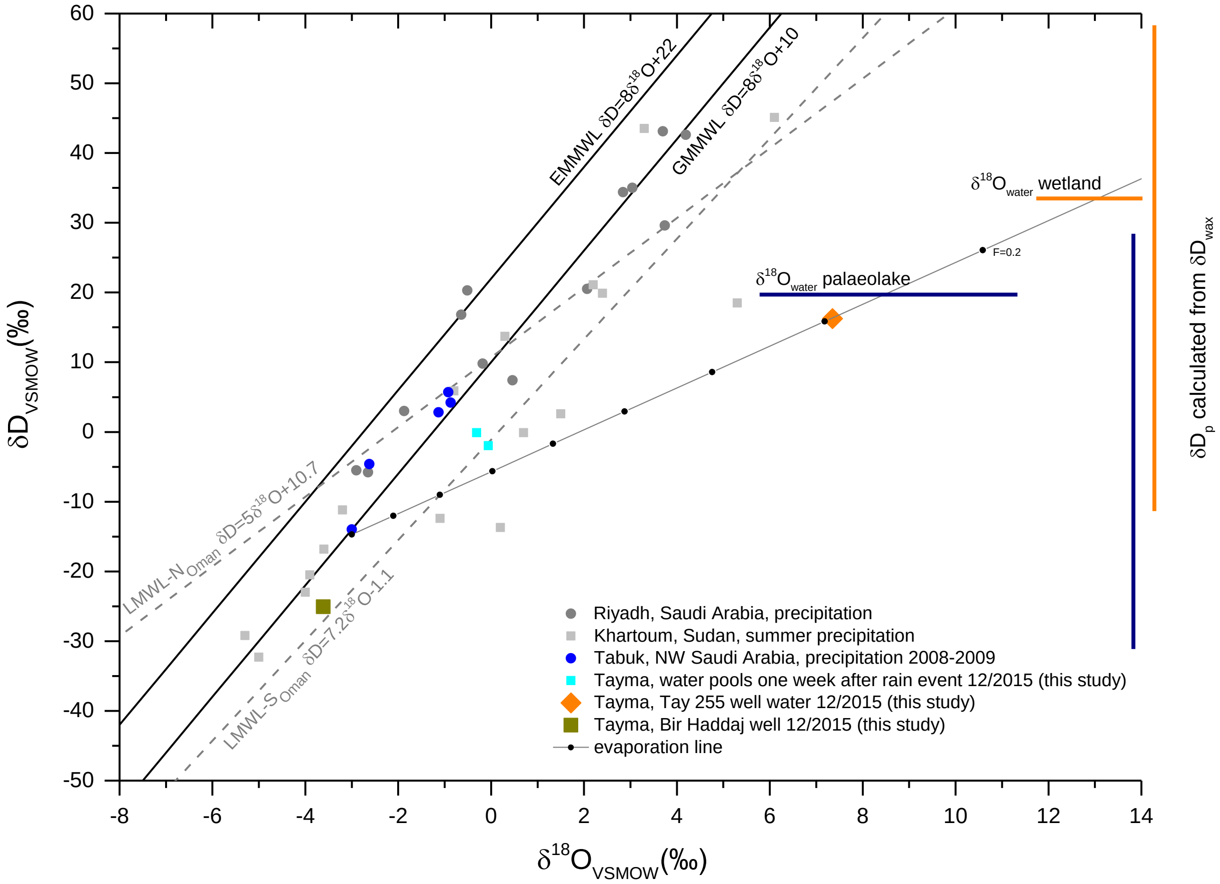

Supplementary Fig. 8: δD and δ^{18}O plot of Tayma palaeolake water and tentative palaeo-moisture source reconstruction. For the isotopic characterisation of moisture sources, we used the Global Meteoric Water Line (GMWL) and Eastern Mediterranean Meteoric Water Line (EMMWL; high δD excess)[16], the two Local Meteoric Water Lines of rainstorm events in Oman[17], with LMWL-N (Mediterranean frontal systems; enriched δD) and LMWL-S (Indian Ocean cyclones and tropical depressions; depleted δD and δ^{18}O), the Red Sea-influenced rainstorm events in Riyadh[18] (partly enriched δD), the composition of the African monsoon precipitation (data from Khartoum, Sudan; partly depleted δD)[19], and few available precipitation data from Tabuk, NW Saudi Arabia[19], very close to Tayma. Surface rainwater collected in water pools in a wadi SW of the Tayma palaeolake show $\delta^{18}O_{water}$ and δD_{water} values of around -0.5‰. The stable isotopes of the Bir Haddaj well in Tayma reflect sub-surface groundwater with -3.5‰ $\delta^{18}O_{water}$ and -24.6‰ δD_{water}, similar to the middle of the Saq aquifer[20,21]. Groundwater sampled at 1.5 m depth in the well of Tay 255 (in 2015) shows highly enriched values of +7.4‰ $\delta^{18}O_{water}$ (+16.2‰ δD_{water}), only slightly lower than the calculated mean $\delta^{18}O_{water}$ of +8.4‰ for the palaeolake surface water between 8,800 and 7,950 cal yr BP. In comparison, the modelled mean $\delta^{18}O_{water}$ of the wetland phase between 7,800 and 6,800 cal yr BP is extremely heavy (+13.1‰). The difference between both settings will be mainly influenced by changes in evaporation, possibly also in precipitation. Past precipitation estimates (δD_p) based on $\delta D_{nC29,\ nC31}$ range between -28 and +44‰ for the deep lake phase and -11 and +58‰ for the wetland phase, which may indicate a change in the predominant atmospheric moisture source. We calculated an evaporation line between $\delta^{18}O_{water}$ = -3‰ for the groundwater-supported lake and +7.4‰ of Tay 255 well water using the Rayleigh equation[22] and found a high evaporation rate of >70% for the surface water of the deep lake and >80% for the shallow lake phase that reflect highly arid conditions.

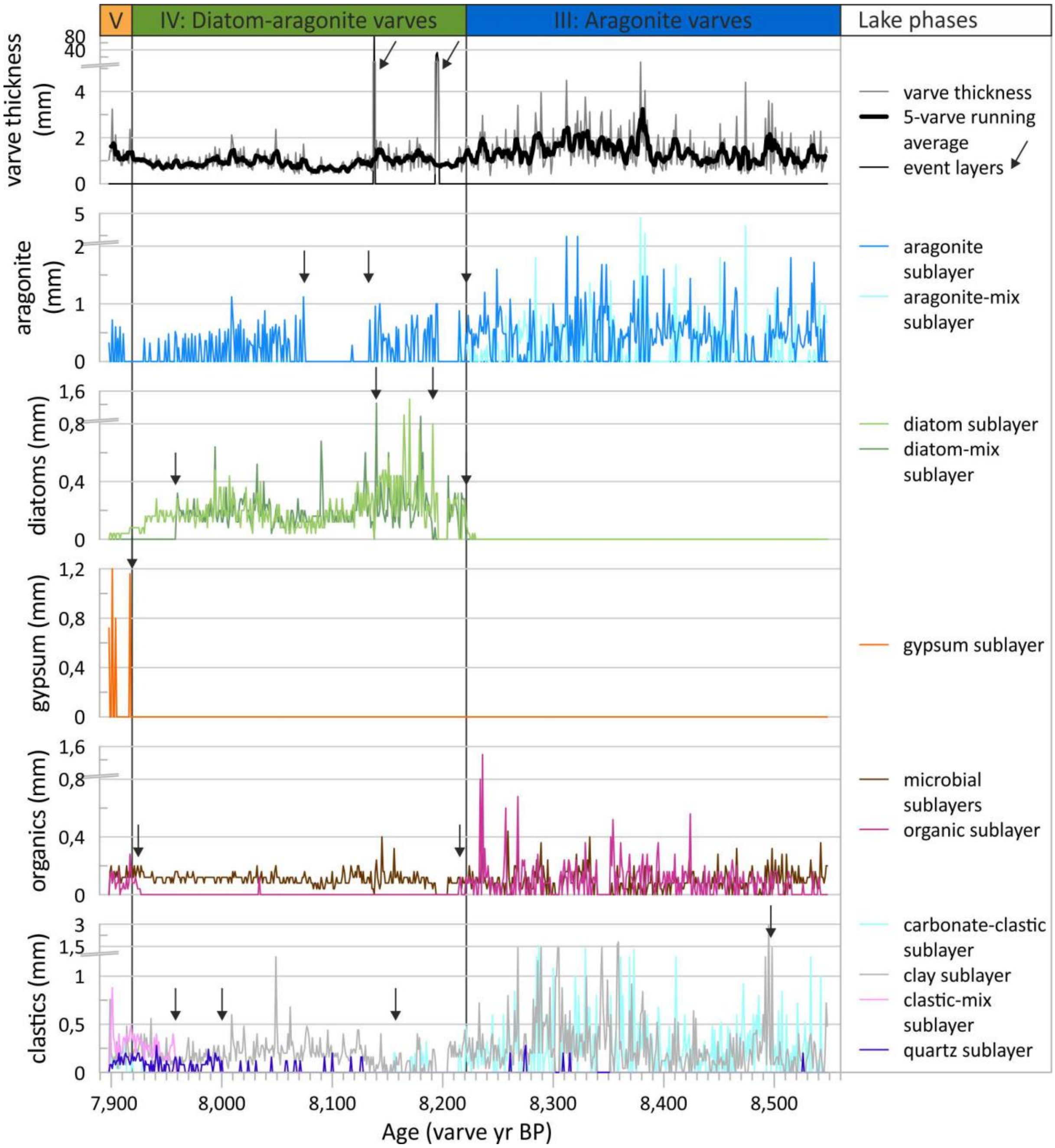

Supplementary Fig. 9: Varve micro-facies of lake phases III (aragonite varves), IV (diatom-aragonite varves) and V (transition to clastic-evaporitic lamination). Each varve (annual lamination) consists of at least two, but mostly three or more sublayers. Black arrows mark two several cm-thick graded event layers in the varve thickness panel (top); in the sublayer panels, arrows point either towards the onset or ceasing occurrence of a sublayer, or to particularly thick sublayers.

References

1. Engel, M. et al. The early Holocene humid period in NW Saudi Arabia – sediments, microfossils and palaeo-hydrological modelling. *Quat. Int.* **266**, 131–141 (2012).
2. Wellbrock, K. et al. in: *Taymāʾ I* (eds. Hausleiter, A., Eichmann, R. & al-Najem, M.) 145–198 (Archaeopress, 2018).
3. Hausleiter, A. & Eichmann, R. in: *Taymāʾ I* (eds. Hausleiter, A., Eichmann, R. & al-Najem, M.) 3–58 (Archaeopress, 2018)
4. Ginau, A., Engel, M. & Brückner, H. Holocene chemical precipitates in the continental sabkha of Tayma (NW Saudi Arabia). *J. Arid Environ.* **84**, 26–37 (2012).
5. Engel, M. et al. Lakes or wetlands? A comment on 'The middle Holocene climatic records from Arabia: Reassessing lacustrine environments, shift of ITCZ in Arabian Sea, and impacts of the southwest Indian and African monsoons' by Enzel et al. *Global Planet. Change* **148**, 258–267 (2017).
6. Barth, H. K. Das arabische Schichtstufenland (zentraler Teil). *Beihefte TAVO, Reihe A (Naturwissenschaften)* **9**, 90–125 (1985).
7. Al-Ahmadi, M. E. Hydrogeology of the Saq aquifer northwest of Tabuk, northern Saudi Arabia. *J. King Abdulaziz Univ. Earth Sci.* **20**, 51–66 (2009).
8. UN-ESCWA & BGR. *Inventory of shared water resources in Western Asia Ch 10* (Beirut, 2013).
9. Al-Najam, M. H. Irrigation system and ancient water resources in Tayma. *ATLAL J. Saudi Arab. Archaeol.* **15**, 191–197 (2000).
10. Wellbrock, K., Strauss, M., Külls, C. & Grottker, M. in: *Des refuges aux oasis: Vivre en milieu aride de la Préhistoire à aujourd'hui. XXXVIIIe rencontres internationales d'archéologie et d'histoire d'Antibes* (eds. Purdue, L., Charbonnier, J. & Khalidi, L.) 231–249 (Éditions APDCA, 2018).
11. Vaslet, D. et al. *Geologic map of the Tayma quadrangle, sheet 27C: Kingdom of Saudi Arabia* (Ministry of Petroleum and Mineral Resources, 1994).
12. Dinies, M., Neef, R., Plessen, B. & Kürschner, H. in *The Archaeology of North Arabia: Oases and Landscapes* (ed. Luciani, M.) 57–78 (Austrian Academy of Sciences Press, 2016).
13. Blaauw, M. & Christen, J. A. Flexible paleoclimate age-depth models using an autoregressive gamma process. *Bayesian Anal.* **6**, 457–474 (2011).
14. Reimer, P. J. et al. IntCal13 and Marine13 radiocarbon age calibration curves 0–50,000 Years cal BP. *Radiocarbon* **55**, 1869–1887 (2013).
15. Neugebauer, I. et al. Implications of S1 tephra findings in Dead Sea and Tayma palaeolake sediments for marine reservoir age estimation and palaeoclimate synchronisation. *Quat. Sci. Rev.* **170**, 269–275 (2017).
16. Gat, J. R. Oxygen and hydrogen isotopes in the hydrological cycle. *Annu. Rev. Earth Pl. Sc.* **24**, 225–262 (1996).
17. Weyhenmeyer, C. E., Burns, S. J., Waber, H. N., Macumber, P. G. & Matter, A. Isotope study of moisture sources, recharge areas, and groundwater flow paths within the eastern Batinah coastal plain, Sultanate of Oman. *Water Resour. Res.* **38**, 1184 (2002).

18. Michelsen, N. et al. Isotopic and chemical composition of precipitation in Riyadh, Saudi Arabia. *Chem. Geol.* **413**, 51–62 (2015).

19. IAEA & WMO. *Global Network of Isotopes in Precipitation. The GNIP Database.* https://nucleus.iaea.org/wiser (2018).

20. Alyamani, M. S. Isotopic composition of rainfall and ground-water recharge in the western province of Saudi Arabia. *J. Arid Environ.* **49**, 751–760 (2001).

21. Al-Sagaby, A. & Moallim, A. Isotopes based assessment of groundwater renewal and related anthropogenic effects in water scarce areas: Sand dunes study in Qasim area, Saudi Arabia. *IAEA-TECDOC* **1246**, 221–229 (2001).

22. Dansgaard, W. Stable isotopes in precipitation. *Tellus* **16**, 436–468 (1964).